FSI-88-TN7

FLOW MODELING FOR CASTING ANALYSIS

C.W. Hirt and R.P. Harper
Flow Science, Inc.
3-10-88

PURPOSE

As part of the fourth conference on "Modeling of Casting and Welding Processes," April 17-22, 1988 in Palm Coast, Florida, a round robin session was proposed in which participants would compare modeling results for a specific casting. Limited experimental data for temperature histories at several locations in the cast were not revealed to the participants until the time of the meeting. No flow data were taken except for the approximate pouring time. The purpose of this session was to provide a comparison between different computer codes with respect to type, user friendliness, display capabilities, etc.

In this technical note we report FLOW-3D results obtained for the fluid dynamic processes involved in the filling of the casting. A thermal analysis of the filled casting has not yet been performed with FLOW-3D.

The casting selected for the round robin session is a hammer head made of 8740 steel and weighing about 65 kg (143 lbs). The casting was made in a sand mold. Figure 1 shows a drawing of the part provided to the participants, while Fig. 2 shows a sketch of the associated sprue and riser used in the casting process.

MODELING ASSUMPTIONS

Because our interest was in studying the flow generated within the mold, we did not attempt to model the sprue or riser. This means, however, that we had to make some assumptions regarding the metal flow entering the mold. In the specifications to participants it was stated that the total pouring time was 15 sec. A personal communication with the organizers indicated that this time corresponded to the total time the pouring ladle was tipped for pouring, and that it varied considerably from one test to another. Since this time included filling the sprue and riser as well as the mold, we must use some other method to estimate the mold filling time. For the present analysis we assumed that the 2 by 2 square inch runner between the sprue and riser was full of metal flowing at 42 in/s, corresponding to approximately a 2.3 inch hydrostatic head in the sprue. This horizontal flow then falls under gravity to enter the mold. Assuming a fall of slightly less than one inch, the vertical flow speed would be 27 in/s. Thus, our model for the flow entering the mold consisted of a steady stream moving with a horizontal speed of 42 in/s and a vertical speed of 27 in/s, and had a horizontal cross section of 4 square inches. Because the flow rate entering the computational mold is 27/42 times smaller than the flow rate passing through the runner from the sprue, this model effectively assumes that the riser is filling at the same time as the mold. This is probably not realistic and suggests that a more accurate model should allow for a time-dependent flow rate into the mold to account for a hydrostatic head buildup in the riser. FLOW-3D can accept time-dependent boundary condition data, but in the absence of more detailed experimental information it does not appear worthwhile to attempt such refinements at this time.

The mold, sprue, and riser have geometric symmetry with respect to a vertical midplane. We assume the flow also remains symmetric so that only one symmetry half of the system has been explicitly modeled.

For flow purposes the only physical property of the metal that is required is its density and for this we have simply used the density of steel at 7.8 g/cc. No physical properties of the sand mold are required. Implicit in these statements is the fact that we have elected to treat the metal flow as one dominated by inertia and have neglected all viscous effects, including wall shear stresses and turbulence. These effects could be included in the FLOW-3D representation, but here again it is not worthwhile adding these complications until more experimental data is available.

FLOW-3D is a finite-difference (i.e., finite-volume) based method in which free surfaces are tracked by a volume-of-fluid method and obstacles are defined by the fractional areas/volumes of each mesh cell that are open to flow. (We refer to this obstacle definition method as FAVOR.) Because the mesh of control volumes used for numerical approximations entails a finite resolution size, there is a limit to the size of geometric details and flow variations that can be resolved. As more detail is sought the total number of mesh cell increases, and this, in turn, increases the computational cost. For the present case we have used a mesh in which some of the smaller corner rounding details are not resolved. Since we are primarily interested in the overall flow patterns and transients generated during the filling process, this approximation to the geometry is not likely to be significant.

MODEL INITIALIZATION

Units of inches, seconds, and mass in units of 12 slugs will be employed throughout. This peculiar mass unit gives pressures in pounds per square inch. We shall also use a Cartesian coordinate system in which the origin is located at the center of the hammer head. The z direction will be vertical so that metal flows into the mold in the negative z direction. The x axis is oriented horizontally and directed toward the handle end of the hammer. The y direction is perpendicular to the largest face of the hammer with its origin at the plane of symmetry. This coordinate system will be referred to in describing the computational results.

The mesh selected for modeling the mold region consisted of 20 zones in the x direction, 7 zones in the y direction, and 20 zones in the z direction. Mesh zones are rectangular, but vary in size. Mesh input data (17 numbers) were chosen to place a couple of grid lines at critical locations where abrupt geometry changes occur. The code's mesh generator automatically located all remaining grid lines to insure the best zoning for the number of cells requested. The total number of zones in the mesh, including boundary cells, is 4356. Plots of the mesh are given in Fig. 3.

Geometry describing the flow region is input to FLOW-3D through a solids modeling feature included in the preprocessor program. Regions are defined through general quadratic functions and coordinate limits. These regions can be combined with Boolean operations to intersect in additive or subtractive ways, and sets of regions can be grouped together to define distinct obstacles. For this application four obstacles were defined using a total of 10 functions (61 input numbers). We did not include the 1/2 inch rounding on the inside corners of the rectangular hole extending into the hammer in the x direction or the 3/16 inch rounding of the smaller, rectangular hole cutting through the face of the hammer in the y direction. Figure 4 shows how the code's graphics plotter interprets the resulting geometry from the fractional areas/volumes generated by the preprocessor. The only problem area is in plotting the small rectangular hole cut in the y direction. Because of the limited mesh resolution in this region, the plotter cuts off two of the edges. An exact representation could be generated by further modifying the mesh to insure that grid lines coincide with the sides of this hole, but this was deemed unnecessary for present purposes.

An asymmetry can be seen in Fig. 4 (left frame) in the head of the hammer where the riser is located. This is caused by a hole cut to accept the incoming molten metal. The total open volume in the mesh, including this hole, was computed by the preprocessor to be 246.1 cubic inches. For numerical reasons (i.e., to enhance stability for larger time-step sizes) the code automatically added 21.13 cubic inches to the volume. This addition is in a few mesh zones where an unfavorable ratio of cell area to volume existed. The addition should have a minimal effect on the computed flow distribution.

A complete input data file for this problem is given in Fig. 5, which includes all physical and computational parameters, the mesh and geometry data, and a series of graphic plot requests. Several of the Namelist input sections are blank as they were not needed. For example, no baffles, initial fluid configurations, or temperature distributions were required.

COMPUTATIONAL RESULTS

To visualize the flow, a series of velocity vector plots will be presented for selected cuts through the mold. All figures will be composites of six plots at times 0.00, 1.00, 2.13, 3.13, 4.08, and 4.87 sec. Time zero corresponds to the beginning of flow into the mold, while the final 4.87 sec time corresponds to complete filling of the mold. At complete filling the calculation failed to converge because no further space was available for the incoming flow.

Flow Structure Near Inlet

First, a word about these plots. Velocity vectors are drawn out from the center of each computational zone that is at least half full of fluid. The direction and length of each vector corresponds to the fluid velocity computed in that zone. No arrowheads are used as these tend to make the plots too busy. Flow directions are easy to determine since the vector bases must line up in straight lines. Free surfaces are indicated by a contour of the volume fraction of fluid equal to one half. Obstacle regions are marked by stars to distinguish them from open regions where there is no fluid.

Because the incoming flow is rapidly spread out into a relatively thin sheet, it does not always fill zones more than half way, which means that these sheets are not plotted. A good example of this is in the region near the inlet. The horizontal component of the incoming fluid causes it to strike the left side of the mold (at x=0) and because of its impact pressure the fluid is given a component of velocity in the positive y direction. Thus, even though the initial width of the entrant flow is 1 inch, it is immediately spread out over the entire 2.25 inch (half) width of the mold. In fact, the y component of momentum is sufficient to cause the flow to splash on and down the y=2.25 face of the mold. The flow in this region is too thin to show up in the standard plots as mentioned above, but we can visualize it somewhat better by asking the plotter program to plot velocities in all cells regardless of the amount of fluid they contain. For example, in Fig. 6 we have done this in the layer of zones adjacent to the x=0 face of the mold. The incoming flow has a width extending only from y=0.0 to y=1.0, but as this plot clearly shows the flow has been diverted across the face toward the y=2.25 wall. It seems likely that the z component of vorticity generated in this complicated flow process and the sending of thin sheets of molten metal over a wide surface area is less than ideal for making good quality castings.

Filling Characteristics

A general idea of how the mold fills can be obtained from Figs. 7-8. In Fig. 7 are plots of the flow history in the plane of mesh zones adjacent to the symmetry plane (y=0). As expected, the flow is always downwards along the left edge because this is where the inlet flow is directed. It is also not surprising that the fluid remains more or less in the bottom of the mold since gravity is the predominant dynamic influence on the liquid metal. An interesting feature associated with the swirl (z-vorticity) of the incoming metal is the fact that, at early times, the fluid level along the left side below the inlet is lower than the fluid level elsewhere. Because of the diversion of fluid onto the y=2.5 wall, a considerable amount of fluid reaches the bottom region away from the left boundary. This is particularly evident in the second frame (t=1.00) of Fig. 7.

As the mold fills we note that the maximum flow velocity in the system decreases (see numbers printed at the top of each frame in Fig. 7). This makes sense because the maximum velocity is generated in the fluid falling under the action of gravity from the riser into the pool forming in the bottom of the mold. With progressive filling the incoming fluid has a shorter distance to fall and is accelerated less.

The three-dimensional nature of the flow is obvious from a comparison of Fig. 7 with Fig. 8, which shows the flow structure in the plane of zones adjacent to the outside surface of the mold. For instance, comparing the second frame in each figure (at t=1.00) we see a depression in the surface at the midpoint horizontally in Fig. 7, while there is a crest in Fig. 8. Similarly, in comparing the fourth frame of each figure we see that the flow has clearly reached a higher elevation over the right half of the mold at the front face (Fig. 8) than it has at the center (Fig. 7). Shortly after the time of this frame this higher fluid spills over the left side of the small rectangular obstacle in the center of the mold. The spilling causes temporary large eddy flows in the lower left pool region.

Although it is not immediately apparent from these plots, a review of additional graphic output shows that there is some horizontal sloshing in the time interval from 1.00 to 2.00 seconds. The sloshing arises from the inertia of the incoming fluid, which initially fills the right half of the mold to a higher level than the left half. Gravity eventually dominates and forces the surface to slosh back to the left creating some transient reverse flow regions and local vortex structures.

Even when the mold has completely filled there are significantly different velocity profiles in the two plots, and this is further evidence for the strong three-dimensional character of the flow.

Secondary Flows

It is tempting to view the mold flow as a nearly two-dimensional process since the mold is relatively thin in the y direction compared to its horizontal and vertical dimensions. Unfortunately, as we have already seen there are significant three-dimensional flow processes. Further evidence for the complicated nature of the flow can be gathered from Fig. 9, which shows flow in the second y-z plane of zones removed from the left wall. The frame times are the same as those in the previous figures. Even a casual review of these plots reveals a highly transient flow behavior involving multiple vortices and sloshing.

A y-z cut through the mold at its far right side, Fig. 10, shows a simpler and more uniform flow pattern. Because this region is not directly affected by the incoming flow, it is not surprising that it exhibits a less complicated flow structure.

For completeness, Fig. 11 contains several plots in the vertical midplane (x-y plane). The second frame at t=1.00 sec shows no flow since the filling has not yet reached this level and the incoming stream along the left side is too thin to be plotted.

DISCUSSION

From the standpoint of casting quality the mold and riser should be configured to eliminate or, at least, minimize any splashing and sloshing that can lead to repeated wetting of mold surfaces, entrainment of air, and possibly even the erosion of the sand mold walls. Ideally, one would like to have a smooth, laminar flow entering and filling the mold.

In the present example, and assuming that our inlet specification is not too unrealistic, we have seen that there are complicated, three-dimensional flow transients taking place with a considerable amount of splashing at early times. This would seem to be less than ideal. Several areas for improvement can be identified from the calculational results. First, having the inlet stream narrower than the mold width leads to the formation of thin sheets of metal splashing onto the outside walls of the mold and the formation of a z component of vorticity. A redesign of the sprue/riser system to include a sluice that spreads the flow out to the width of the mold would eliminate this adverse flow process.

Second, having the mold arranged with its maximum dimension vertical and the riser located at the topmost point, the incoming flow is given the maximum opportunity for acceleration to high velocities. This in turn leads to more splashing and sloshing than necessary. By alternatively arranging the mold in a horizontal position with its smallest dimension vertical, high flow velocities would be largly eliminated and would considerably reduce the amount of splashing.

Lastly, both the narrow incoming stream and the vertical arrangement of the mold contribute to strong three-dimensional flow structures, for example, the spilling of the flow over the interior rectangular obstacle shortly after t=3.13 sec, and the complicated, transient eddy behavior in the lower left corner of the mold throughout the entire filling process.

These observations are of a qualitative nature and it is clear that a considerable amount of work has yet to be done to understand how to interpret the computed results in terms of real castings. Nevertheless, it should also be clear that computational results like those from FLOW-3D can provide an enormous amount of detailed information, which is not easily obtainable by any other means.

COMPUTATIONAL REQUIREMENTS

It is estimated that the initial model development time, that is, the time necessary to generate the input data file for FLOW-3D, was about three to four hours. Most of this time was consumed in making decisions about the amount of detail to include (for example, how to model the inflow) and in calculating the function coefficients describing the geometry.

All results presented here were obtained with the FLOW-3D program running in double precision on a MicroVAX II computer. The latest version of the code, Version-88, was used while still in a shakeout period before its release. For this reason some intermediate results (the calculations were run in several segments) were found to have errors and had to be repeated, which makes it difficult to quote an exact CPU time for the entire calculation. We estimate that the time required using the final Version-88 code should be on the order of 42 hours. This time depends strongly on the resolution selected for the calculations and on the rate at which metal is specified to flow into the mold.

Computational time also has a strong dependence on the size of computer used for the analysis. The MicroVAX II is not an especially fast machine. For instance, some current workstation machines of comparable cost are reputed to operate at speeds several times faster. In any case, this computational time is not unreasonable considering the amount of information obtained.

Flow Science, Inc.
1325 Trinity Drive
Los Alamos, New Mexico 87544
505-662-2636

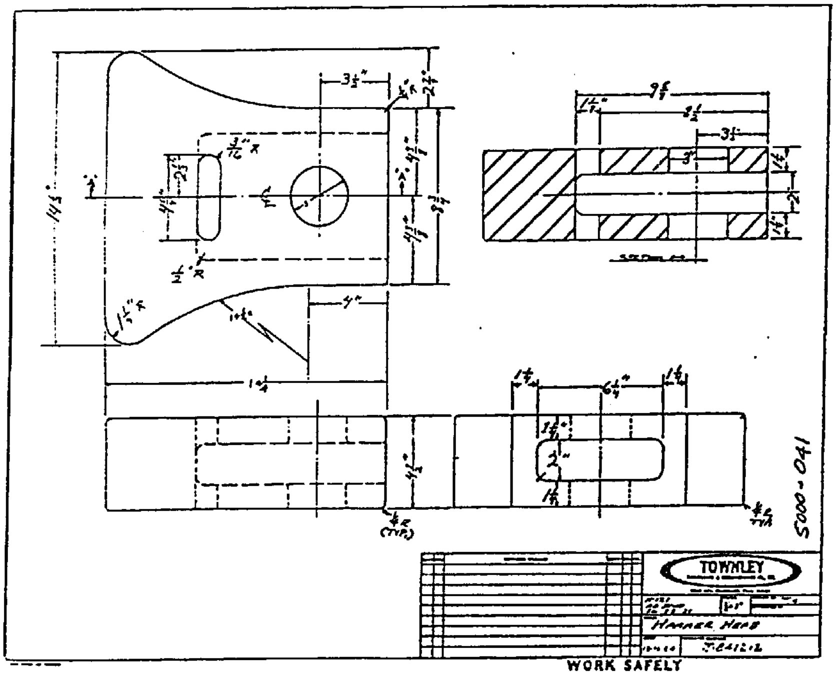

Fig. 1. Engineering drawing of part to be cast.

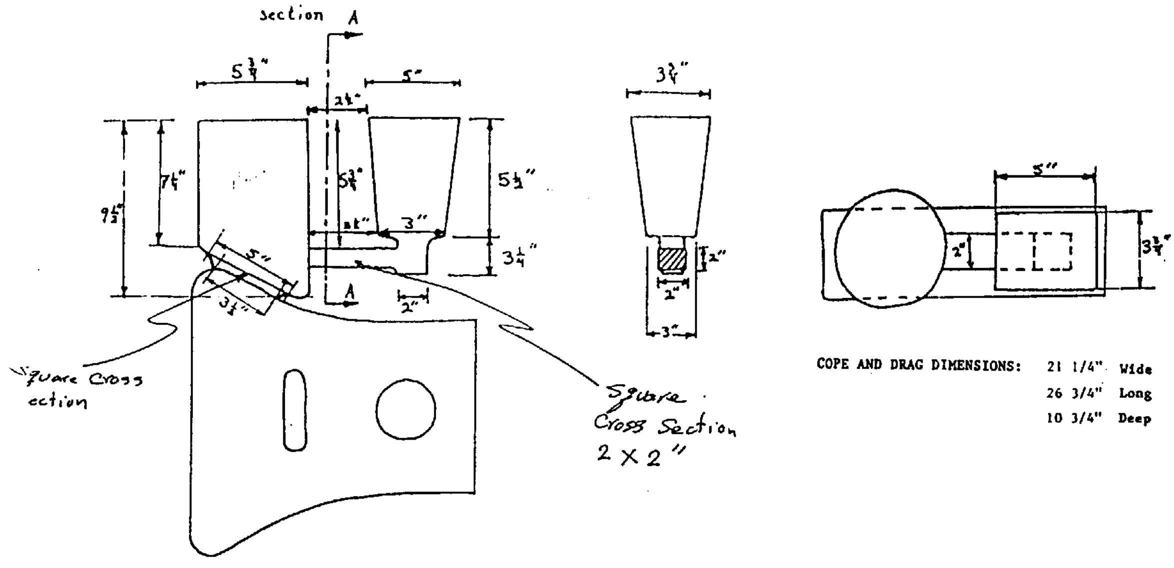

Fig. 2. Schematic of sprue and riser in relation to part.